



Title	Evaluating Strategies to Normalise Biological Replicates of Western Blot Data
Authors(s)	Degasperi, Andrea, Birtwistle, Marc R., Volinsky, Natalia, Kolch, Walter, Kholodenko, Boris N.
Publication date	2014-01-27
Publication information	Degasperi, Andrea, Marc R. Birtwistle, Natalia Volinsky, Walter Kolch, and Boris N. Kholodenko. "Evaluating Strategies to Normalise Biological Replicates of Western Blot Data." PLOS, January 27, 2014. https://doi.org/10.1371/journal.pone.0087293 .
Publisher	PLOS
Item record/more information	http://hdl.handle.net/10197/5844
Publisher's statement	This is an open-access article distributed under the terms of the Creative Commons Attribution License, which permits unrestricted use, distribution, and reproduction in any medium, provided the original author and source are credited.
Publisher's version (DOI)	10.1371/journal.pone.0087293

Downloaded 2026-05-01 23:34:58

The UCD community has made this article openly available. Please share how this access benefits you. Your story matters! (@ucd_oa)



© Some rights reserved. For more information

1 **Evaluating Strategies to Normalise Biological Replicates of Western Blot Data**

2 Andrea Degasperi^{1,c}, Marc R. Birtwistle², Natalia Volinsky¹, Jens Rauch¹, Walter Kolch^{1,3,4} and Boris N.
3 Kholodenko^{1,3,4}

4 ¹Systems Biology Ireland, Conway Institute, University College Dublin, Belfield, Dublin 4, Republic of Ireland

5 ²Icahn School of Medicine at Mount Sinai, Dept. of Pharmacology and Systems Therapeutics, One Gustave L.
6 Levy Place, Box 1603, New York, NY 10029, USA.

7 ³ Conway Institute of Biomolecular & Biomedical Research, University College Dublin, Belfield, Dublin 4,
8 Ireland

9 ⁴ School of Medicine and Medical Science, University College Dublin, Belfield, Dublin 4, Ireland

10

11 ^c Corresponding author, e-mail address: andrea.degasperi@ucd.ie

12

13 **Abstract**

14 Western blot data are widely used in quantitative applications such as statistical testing and mathematical
15 modelling. To ensure accurate quantitation and comparability between experiments, Western blot replicates
16 must be normalised, but it is unclear how the available methods affect statistical properties of the data. Here we
17 evaluate three commonly used normalisation strategies: (i) by fixed normalisation point or control; (ii) by sum
18 of all data points in a replicate; and (iii) by optimal alignment of the replicates. We consider how these different
19 strategies affect the coefficient of variation (CV) and the results of hypothesis testing with the normalised data.
20 Normalisation by fixed point tends to increase the mean CV of normalised data in a manner that naturally
21 depends on the choice of the normalisation point. Thus, in the context of hypothesis testing, normalisation by
22 fixed point reduces false positives and increases false negatives. Analysis of published experimental data shows
23 that choosing normalisation points with low quantified intensities results in a high normalised data CV and
24 should thus be avoided. Normalisation by sum or by optimal alignment redistributes the raw data uncertainty in
25 a mean-dependent manner, reducing the CV of high intensity points and increasing the CV of low intensity
26 points. This causes the effect of normalisations by sum or optimal alignment on hypothesis testing to depend on
27 the mean of the data tested; for high intensity points, false positives are increased and false negatives are
28 decreased, while for low intensity points, false positives are decreased and false negatives are increased. These
29 results will aid users of Western blotting to choose a suitable normalisation strategy and also understand the
30 implications of this normalisation for subsequent hypothesis testing.

31

32 **Introduction**

33 Western blotting or protein immunoblotting, was introduced at the end of the 1970s to enable the detection of
34 specific proteins [1,2]. Although originally a qualitative or at best a semi-quantitative method, with the rise of
35 computational systems biology [3], Western blotting has become increasingly important for fully quantitative
36 applications. Two main applications are the parameterisation and validation of mathematical models of
37 biological systems [4] and the testing of statistical significance between two or more experimental conditions or
38 treatments [5].

39 Although technical aspects of Western blotting have improved over the years, for example by extending the
40 linear range of detection [6], it is not yet clear how much quantitative information can be obtained and in which
41 settings. Here we investigate the quantitative use of Western blotting, to determine its applicability and limits

42 depending on the detection method and the data normalisation strategy used to quantitatively compare biological
43 replicates of the same experimental conditions.

44 A requirement for the quantitative use of Western blot data is the linearity between quantified intensities and
45 protein amounts. To detect and correct non-linearity, the authors in [7] suggest to use hyperbolic calibration
46 curves to interpolate the correct relative concentration of the proteins of interest. These are dilution curves that
47 need to be treated simultaneously to samples of interest, and in most situations constructing these dilution curves
48 is not practical. Because this method is highly labour consuming and is not a laboratory common practice, we do
49 not consider this approach in this paper. Nonetheless we investigate linearity in our Results section, where we
50 quantify the extent of the linear range in the case of two detection systems: enhanced chemiluminescence (ECL)
51 with X-ray film and ECL with charge coupled device (CCD) imager.

52 Although the topic of data normalisation has been widely explored in the context of microarrays [8], it has not
53 yet been fully investigated in the context of Western blotting. For microarrays, such as single channel
54 oligonucleotide arrays, the issue of data normalisation arises naturally when expression indices, obtained from
55 gene probe sets intensities, need to be compared across different arrays, for example to identify differentially
56 expressed genes [9]. In order to compare arrays quantitatively, several normalisation strategies have been
57 proposed, where expression indices or intensities are scaled or transformed depending on the assumptions
58 underlying each strategy. For example, assuming that the total amount of sample RNA is constant across arrays,
59 the intensities are scaled such that the sum or the average of all intensities is equal across arrays (scaling
60 methods [9]). Alternatively, assuming that the distribution of the intensities is conserved across arrays, the data
61 is transformed such that the quantile-quantile plot of the intensities of the arrays approaches a straight line
62 (quantile normalisation [9]). Or again, assuming that there is a set of genes whose expression index does not
63 change across arrays, such as a set of housekeeping genes, this set can be used as reference (invariant set
64 normalisation [10]).

65 In the case of Western blotting, usually a single protein is measured and a limited number of experimental
66 conditions is on the same blot and is detected at the same time; a situation in stark contrast to microarrays where
67 thousands of gene expression measurements are obtained for potentially many more conditions than is typically
68 done by Western blotting. The data or measurements from a Western blot are obtained by dividing quantified
69 intensities (optical densities – OD) by the intensities of appropriate reference proteins, e.g. housekeeping
70 proteins, from the same samples. This procedure adjusts the intensities with respect to small variations in the
71 number of cells and loading across samples within the same blot [11-13]. The need to normalise the data arises
72 when comparing the results from biological replicates of the same experiment, for example to obtain statistical
73 evidence that different conditions induce different protein amounts. We classify Western blot normalisations
74 into three categories. The first and most widely used normalisation method is normalisation by fixed point
75 (Figure 1A). It divides the data of a replicate by the measurement of a single condition, often referred to as
76 control. It should be noted that although this shares similarities with the invariant set normalisation in the
77 context of microarrays, the assumption that the reference condition is constant is not used and is in practice not
78 satisfied. Thus the biological variability of the reference condition influences the variability of the normalised
79 data. The second normalisation category we consider is normalisation by sum (Figure 1B), where the data on a
80 blot is divided by the sum of the data on the same blot [14], or equivalently the data is scaled such that the
81 average is the same across blots [15,16]. It should be noted that in contrast with the analogous normalisation
82 used in microarrays (scaling methods), in this case the sum is not assumed to be a constant. The biological
83 variability of the sum and its dependency on the individual measurements might influence the variability of the
84 normalised data. Most importantly, it is possible to compare two blots only if they present exactly the same
85 conditions, using different lysates derived from cells cultured and treated in the same way. Yet, this condition is
86 regularly met when producing a biological replicate. In our statistical formalisation we address the problem of
87 characterising how the choice of reference (fixed point or sum) influences the normalised data. As third
88 category we consider normalisation by optimal alignment (Figure 1C), where data from replicates are aligned
89 using optimisation algorithms to minimise the uncertainty of the normalised data. Examples of this
90 normalisation minimise either the sum of the squared differences between the replicates of each data point [17]

91 or the coefficient of variation (CV) of the normalised data [18]. The assumption behind this method is that the
92 measurements across replicates should preserve an overall trend.

93 To avoid the need for data normalisation, approaches for the absolute quantification of protein concentrations
94 using Western blotting have been investigated [7,19]. However, these methods are not widespread mainly due to
95 increased experimental effort, in particular the need for purified proteins as standards. It is also possible to
96 obtain replicates of lysates that are directly comparable by means of multi-strip Western blotting [20], where
97 replicates are cut from different gels and blotted on the same membrane. However, multi-strip Western blots are
98 typically used to compare more conditions on the same membrane, rather than replicates.

99 The quantitation of Western blots has also been the subject of theoretical investigations. In [21] the authors use a
100 large amount of data to identify a suitable error model for Western blot data. Using the error model, they dissect
101 the different sources of error, concluding that the main sources of variability are multiplicative and so log-
102 normally distributed. Additionally, by removing the sources of error, they reduce the variability in the data
103 significantly. This work is based on error models for microarray data [22], and is applicable only when a large
104 amount of data is available. In [19], the authors suggest that technical errors can be reduced using a
105 randomisation of time courses on a gel and smoothing the data using spline regression.

106 In this paper, first we discuss the problem of linearity between protein concentrations and quantified optical
107 densities, which is a fundamental prerequisite to use Western blot data quantitatively in the absence of hard-to-
108 obtain calibration curves. Second, we investigate how the choice of the normalisation strategy affects the
109 normalised data. In particular, we evaluate the normalisations in terms of their ability to reduce variability in the
110 data and of how they affect statistical decisions.

111 **Materials and Methods**

112 **Sample Preparation**

113 The MCF-7 cell line was maintained under standard conditions in Dulbecco's modified Eagle's medium
114 supplemented with 10% foetal bovine serum. Cells were washed with ice cold phosphate buffered Saline and
115 lysed in RIPA buffer (1% NP-40, 0.1% SDS, 0.5% Sodium deoxycholate, 50 mM Tris pH 7.5, 150 mM NaCl)
116 supplemented with protease and phosphatase inhibitor cocktails (Sigma Aldrich) and protein concentration was
117 quantitated by BCA protein assay (Invitrogen). Purified BSA (Applichem) was dissolved in RIPA buffer. Cell
118 lysates and a BSA sample were serially diluted 1:2 and run on SDS-PAGE using a standard protocol. Proteins
119 were transferred to the PVDF (for ECL based detection) or Nitrocellulose (for LI-COR based proteins detection)
120 membranes. Membranes were blocked with blocking solution (11500694001, Roche) for BSA detection or 5%
121 skimmed milk for rest of the membranes. For Western blotting ERK (M-5670, Sigma Aldrich), mTOR (2972,
122 Cell Signaling Technology), RSK1 (sc-231, Santa Cruz) and BSA (sc-50528, Santa Cruz) antibodies were used.
123 Anti-rabbit HRP-conjugated (Cell Signaling Technology) or anti-Rabbit IR 800 (LI-COR) secondary antibodies
124 were used for ECL or LI-COR protein detection systems, respectively. Signal was detected by standard X-ray
125 films (Fuji), CCD camera (Advanced Molecular Vision) or LI-COR scanner.

126 **Image Acquisition and Densitometry**

127 Several exposure times were tested for both ECL with film and ECL with CCD imager. In the case of the CCD
128 imager we could choose the longest exposure that presented no signal saturation (overexposure), as detected by
129 the software used in combination with the imager. In the case of X-ray film, we used our experience to select the
130 films that had a good compromise between number of bands visible and the least possible exposure time. Films
131 were digitalised using a high resolution CCD scanner (EPSON Perfection v750 Pro) without additional image
132 corrections that could alter the linearity, such as automatic gain control [23]. Densitometry analysis was
133 performed using the ImageJ Gel Analysis tool, where gel background was also removed individually for each
134 band.

135 **Statistical Analysis of the Dilution Experiments**

136 To assess the linearity of the dilution experiments we used linear regression and computed the coefficient of
137 determination R^2 using Microsoft Excel software. Briefly, the closer the coefficient of determination is to 1,
138 the more the linear model is appropriate to represent the data. For each detection method we tested different
139 dilution ranges by determining R^2 using the first n visible bands, i.e. starting from the least intense band that
140 could be detected. For example, to test the linearity of the five dilutions range, reflecting a 32 fold difference,
141 we computed the linear regression of the first six ($n=6$) visible bands of a dilution curve and computed R^2 . We
142 then computed R^2 independently for three replicates and obtained mean and standard error. Using this
143 approach we could compare coefficients of determination for specific dilution ranges across different detection
144 methods. All quantified coefficients of determination of the dilution experiments can be found in Supporting
145 Information S3.

146 **Theoretical Analysis of Normalisation Procedures**

147 The theoretical analysis was performed developing dedicated scripts in the R language for statistical computing
148 and implementing dedicated C++ programs. While R was used mainly to compute the results inferred from
149 Western blot data, shown in Figures 3C, 4, and Supporting Information Figure S8, C++ programs were used to
150 compute the results in the theoretical scenarios. To obtain samples from log-normal distributions, we computed
151 samples from normal distributions using the Box-Muller method [24] and then exponentiated these samples with
152 base e . Mean and variance of these normal distributions were calculated so that the mean and variance of the
153 log-normal distributions were as desired (Figure 3A). Combining samples from log-normal distributions we
154 could obtain samples from the distributions of the normalised data, as defined in the text (Equations (2), (4) and
155 (8)). Because the log-normal distributions were defined *a priori*, we could then estimate false positives and false
156 negatives results by using t-tests as described in the legend of Figure 5. Briefly, a false positive is defined as a t-
157 test result that yields a p-value lower than 0.05 when testing samples from two distributions that we defined as
158 identical (Figure 5A), while a false negative is defined as a t-test result that yields a p-value greater than 0.05
159 when testing samples from two distributions that we defined as different (Figure 5B). Source files are available
160 upon request from the corresponding author.

161 **Results**

162 **Linearity between Protein Concentration and Quantified Optical Densities**

163 In the absence of a calibration curve, a pre-requisite for obtaining quantitative Western blot data is a linear
164 relationship between the amount of analyte and the measured intensity. To evaluate the extent of the linear range
165 in commonly used detection methods, we prepared two 12 step 2-fold dilution series spanning a 2048-fold
166 concentration range (three independent experiments). One sample series contained isolated Bovine Serum
167 Albumin (BSA) while the other MCF-7 cell lysate. We used the first dilution series to quantify BSA and the
168 second to quantify proteins across a mass range; they included Extracellular signal Regulated Kinases 1 and 2
169 (ERK1/2), ca. 40 kDa, Ribosomal protein S6 Kinase alpha-1 (RSK1), ca. 80 kDa, and Mammalian Target Of
170 Rapamycin (mTOR), ca. 290 kDa. Proteins were detected using two detection systems: ECL with X-ray film
171 and ECL with a CCD imager. Representative experiments with corresponding quantifications can be found in
172 Figure 2 (BSA) and in Supporting Information Figures S1 (ERK), S2 (RSK1) and S3 (mTOR).

173 In order to identify the linear range of a dilution curve we used linear regression for an increasing number of
174 data points, starting from the first detectable and least intense band of a curve. For each regression we then
175 computed the coefficient of determination R^2 , which indicates if the linear regression is a good model for the
176 portion of the curve considered. The closer R^2 is to 1, the more linear the data is. After computing R^2 for each
177 of three replicates we obtained mean and standard error.

178 As expected, our results show that both ECL with X-ray film and with CCD imager have a limited linear range.
179 For example, the full dilution curve of BSA detected with ECL with CCD imager has an R^2 of
180 0.788 ± 0.035 .

181 Interestingly, we found that the linear range of ECL with CCD imager spans about five dilutions (32 fold). In
 182 particular, for all four proteins considered we obtained a significant reduction in R^2 when we consider six
 183 dilutions (64 folds), with respect to five dilutions. For example, in the case of BSA, the coefficient of
 184 determination for five dilutions is 0.994 ± 0.001 , while for six dilutions it is reduced to 0.952 ± 0.011 ,
 185 while for ERK the reduction is from 0.993 ± 0.003 to 0.954 ± 0.01 .

186 ECL with X-ray film presented a smaller linear range than with CCD imager. In particular, for the five dilutions
 187 range where CCD imager is linear, X-ray film yields a sensibly lower R^2 . For example, for the BSA dilution
 188 this is reduced to 0.830 ± 0.023 , while for ERK to 0.732 ± 0.025 . Linearity in the case of ECL with X-ray
 189 film seems to hold only for two or three dilutions, i.e. four or eight fold (Supporting Information S3).

190 The difference between the two systems based on ECL is most likely due to saturation of the X-ray film by high
 191 intensity samples while trying to detect also the lowest intensity samples. This limitation can be avoided using a
 192 CCD imager, which uses a computerised image acquisition system, and is able to detect low intensity signals
 193 without high intensity signals becoming saturated as quickly as with film. Because we were able to avoid this
 194 overexposure, the non-linearity observed using the CCD imager (Fig. 3B) is likely due to antibody interactions,
 195 as suggested in [7].

196 Finally, we investigated the extent of the linear range when using secondary fluorescent antibodies of LI-COR
 197 to detect BSA and ERK (Supporting Information Figure S4). Results were comparable to what we described
 198 above for ECL with CCD imager.

199 In conclusion, the use of ECL with X-ray film for quantitative Western blotting should be limited to the case in
 200 which the intensities vary experimentally not more than 4 to 8 fold. ECL with CCD imager or secondary
 201 fluorescent antibody presents a wider linear range of about 32 fold.

202 **Formalisation of Normalisation Strategies for Western Blot Data**

203 We now move the focus to the evaluation of the normalisation strategies that we categorised in the introduction.
 204 In this section we introduce a formalisation, i.e. a mathematical description, of the normalisation strategies we
 205 investigate. Without loss of generality, consider the measurements of a single target (e.g. a protein) under
 206 different conditions or treatments (e.g. inhibitors, stimuli) on the same blot. Each data point d_i^j , is indexed by
 207 the condition $i \in I$ and the blot replicate number $j \in J$. The standard experimental setups described above
 208 dictate the following:

- 209 1. Data points on one blot are comparable to one another, even if they come from different gel strips [20].
 210 That is, d_i^j with different i but with the same j are directly comparable;
- 211 2. Data points on two different blots are not comparable. That is, d_i^j with different j are not directly
 212 comparable. Normalisation must be employed to enable direct comparison across replicates.

213 Given the linearity conditions explored above are met and that the data points d_i^j are samples from random
 214 variables D_i^j , we have:

$$D_i^j = \alpha_j \cdot [S]_i \quad \forall i \in I, \forall j \in J \quad (1)$$

215 where $[S]_i$ is the concentration of the protein of interest S in condition i , and α_j is the constant of
 216 proportionality of replicate j . Note that if the replicates had been blotted on the same membrane using multi-
 217 strip Western blotting, all the data would be comparable with $\alpha_j = \alpha$ for all $j \in J$.

218 The distribution of $[S]_i$ depends on the mean of the concentration of S across a large number of cells in the
 219 lysate, on the biological variability, and on the technical error. We will now introduce the formalisation of the
 220 normalisation by fixed point or control, by sum of the replicate, and by optimal alignment of the replicates.

221 **Normalisation by a Fixed Normalisation Point or Control**

222 In the normalisation by fixed normalisation point or control a band on the blot common to all replicates is
 223 chosen to be the normalisation point, and the data from a replicate are divided by the value of the normalisation
 224 point. In general, this normalisation can be applied choosing any band that is present on all replicates that need
 225 to be compared. The term ‘‘control’’ usually indicates the band of the untreated or neutral condition. Formally,
 226 this normalisation is a data transformation where the data points d_i^j are substituted by the normalised data
 227 points $\tilde{d}_{i,np}^j$ defined as:

$$\tilde{d}_{i,np}^j = \frac{d_i^j}{d_{np}^j} \quad \forall i \in I, \forall j \in J \quad (2)$$

228 Where the index np indicates a chosen normalisation point, which is an experimental condition all normalised
 229 data become relative to. In terms of random variables, the $\tilde{d}_{i,np}^j$ are samples from the random variables $\tilde{D}_{i,np}^j$
 230 defined as:

$$\tilde{D}_{i,np}^j = \frac{D_i^j}{D_{np}^j} = \frac{\alpha_j \cdot [S]_i}{\alpha_j \cdot [S]_{np}} = \frac{[S]_i}{[S]_{np}} \quad \forall i \in I, \forall j \in J \quad (3)$$

231 Notice that the random variable $\tilde{D}_{np,np}^j$ assumes value 1 with probability 1. Most importantly, the $\tilde{d}_{i,np}^j$ are now
 232 comparable across replicates j , because the constants of proportionality α_j are all cancelled out. Additionally,
 233 all normalised data is dependent on the distribution of the normalisation point. In the following sections we will
 234 show how this dependency influences the variability of the normalised data and we will investigate how to
 235 choose a normalisation point.

236 **Normalisation by Sum of all Data Points in a Replicate**

237 In the normalisation by sum, each data point on a replicate is divided by the sum of the values of all data points
 238 in that replicate. This way the data in each replicate becomes relative to this sum. It is important to ensure
 239 consistency of the sum across replicates, that is exactly the same conditions need to be part of the sum. This
 240 ensures that each data point is divided by a sample that comes from the same random variable. For example, in
 241 the presence of missing values, data points to be summed are chosen so that no replicate of the corresponding
 242 condition has a missing value. Without loss of generality, in this section we give a formalisation of
 243 normalisation by sum where we do not consider missing values.

244 In this normalisation, data points d_i^j are divided by the sum of all data points in a replicate j . Formally, the
 245 normalised data \tilde{d}_i^j are defined as:

$$\tilde{d}_i^j = \frac{d_i^j}{\sum_{k \in I} d_k^j} \quad \forall i \in I, \forall j \in J \quad (4)$$

246 In terms of random variables, the normalised data points \tilde{d}_i^j are samples from the random variables \tilde{D}_i defined
 247 as:

$$\tilde{D}_i = \frac{D_i^j}{\sum_{k \in I} D_k^j} = \frac{\alpha_j \cdot [S]_i}{\alpha_j \cdot \sum_{k \in I} [S]_k} = \frac{[S]_i}{\sum_{k \in I} [S]_k} \quad \forall i \in I, \forall j \in J \quad (5)$$

248 Similar to the normalisation by fixed point, the constants of proportionality α_j cancel and comparable
 249 normalised data are obtained. Notice that the normalised data are dependent on the value of all the data points in
 250 a replicate. The effects of this dependency on the variability of the data and hypothesis testing are investigated
 251 in the following sections. We note that Eq. 5 may be obtained by formulating the normalisation as an
 252 optimisation problem (see Supporting Information S1, Section S1).

253 Normalisation by Optimal Alignment of the Replicates

254 In the normalisation by optimal alignment, the objective is to scale the data by a scaling factor for each replicate,
 255 so that replicates are aligned, that is the distance between data across replicates is minimal. This procedure has
 256 the specific goal of minimising the variability of the normalised data. Moreover, different notions of distance
 257 can be used, yielding different definitions of objective functions. The objective functions formalise the distance
 258 between the data in the replicates and are parametric with respect to the scaling factors. Finding the minimum of
 259 an objective function implies identifying optimal scaling factors. Examples of objective functions are as the sum
 260 of the squared differences between replicates [17] or the mean CV of the normalised data [18]. In the following
 261 we give a formal definition of normalisation by optimal alignment, considering a specific definition of distance,
 262 i.e. the sum of squared differences between replicates.

263 In this normalisation, each replicate j is scaled by a factor β_j so that an optimal alignment of the replicates is
 264 achieved. It is necessary to avoid the trivial solution $\beta_j = 0$ for all $j \in J$, which can be done by introducing
 265 the constraint $\beta_1 = 1$ and estimating the remaining β_j . Here we consider the normalisation by least squared
 266 difference, defined as follows. Assuming we have $|J|$ replicates and we want to align every replicate to the first
 267 replicate, the objective function for a least squared optimal alignment is as follows:

$$268 \quad obj(\beta_2, \dots, \beta_{|J|}) = \sum_{j \in J \setminus \{1\}} \sum_{i \in I} (\beta_j \cdot d_i^j - \beta_1 \cdot d_i^1)^2, \text{ with } \beta_1 = 1$$

269 We minimise obj to find the optimal $\beta_2, \dots, \beta_{|J|}$. The result of this optimisation can be computed analytically
 270 and yields (see Supporting Information S1, Section S2 for the derivation):

$$\beta_j = \frac{\sum_{i \in I} (d_i^1 \cdot d_i^j)}{\sum_{i \in I} (d_i^j)^2} \quad \forall j \in J \quad (7)$$

271 The normalised data \tilde{d}_i^j are defined as follows:

$$\tilde{d}_i^j = d_i^j \cdot \beta_j = d_i^j \cdot \frac{\sum_{k \in I} (d_k^1 \cdot d_k^j)}{\sum_{k \in I} (d_k^j)^2} \quad \forall i \in I, \forall j \in J \quad (8)$$

272 Notice that because of the definition of the β_j , a normalised data point depends on a combination of the value
273 of the data in the same replicate and the value of the data in replicate 1. More complex normalisations by
274 optimal alignment of the replicates, such as the normalisation by minimisation of the mean CV of the
275 normalised data in [18], may present normalised data points that are dependent on the values of all the data. For
276 illustration purposes we use here normalisation by least squared difference as a representative of the
277 normalisations by optimal alignment. We show in the Supporting Information S1, Equation (S5), that the data
278 points normalised by least squared difference are all in the same unit, and are therefore directly comparable. In
279 the next sections we investigate how the normalisations discussed above influence data variability and the
280 statistical inference on data.

281 **Impact of Normalisation on Data Variability**

282 A major aim of data normalisation is to make replicates suitable for quantitative comparison, while ensuring
283 data integrity and avoiding adding uncertainty to the data. Here we show how different normalisation strategies
284 affect the variability of the normalised data. We use the CV of the normalised data to compare the variability
285 that results from applying the different normalisations.

286 For a theoretical investigation of how the choice of normalisation strategy affects the data, we use a simulated
287 scenario. Suppose that the data of eight conditions or treatments is given as in Figure 3A. We chose a data
288 distribution where the response to the treatments from one to eight has an increasing mean but the same CV of
289 0.2. In this and further analyses, we consider these distributions to be log-normal, because of the finding in [21]
290 that the main sources of variability in Western blot data are multiplicative, and therefore log-normally
291 distributed. In the Supporting Information S1, Section S3 and Figures S6 and S7, we replicate the results in this
292 paper using normal distributions and obtain nearly identical results.

293 In Figure 3B we show how normalisation by fixed point, normalisation by sum and normalisation by least
294 squared difference affect the CV of the eight conditions. To obtain these results we estimated the distributions
295 associated with the random variables that we identified in Equation (3), Equation (5) and in the Supporting
296 Information S1, Equation (S5), using a sampling approach based on the Box Muller sampling method [24]. We
297 chose Condition 1 as the normalisation point for the normalisation by fixed point. It should be noted that
298 because every condition is distributed with the same CV, this choice is an invariant in our analysis. The mean of
299 the normalisation point does not determine the CV of the normalised data (data not shown), while we will show
300 below that the CV of the normalised data depends strictly on the CV of the normalisation point chosen and that
301 in practice data points with low mean, i.e. low OD, usually present higher CV. Normalisation by fixed point
302 induced an increase in the mean CV, from 0.2 to 0.25, while increasing equally the CV of the response to each
303 condition, with the obvious exception of Condition 1. Normalisation by sum slightly reduced the mean CV,
304 from 0.2 to 0.196, while the effect on the single responses to the conditions is a redistribution of the CV in a
305 way that is dependent on the mean of the conditions. Conditions with high mean present a reduced CV, while
306 conditions with low mean present an increased CV (albeit slightly). This redistribution is due to the fact that the
307 distribution of the data normalised by sum is dependent on the distribution of all the conditions, as can be seen
308 in Equation (5). Normalisation by least squared difference optimisation increased very slightly the mean CV,
309 from 0.2 to 0.206, while the effect on the single responses to the conditions is a redistribution of the CV
310 analogous to what is observed for the normalisation by sum.

311 In order to obtain evidence that support the above theoretical investigation, we apply the normalisations to our
312 Western blot data published in Supplementary Figure S3 of [25] and also available in Supporting Information
313 Figure S5. These data are composed of two data sets, one with measurements of phosphorylated ERK (ppERK),
314 and the other with measurements of phosphorylated Akt (pAkt). Each data set is composed of three replicates of
315 multi-strip Western blots, where on each blot there are 70 conditions divided into seven time courses for two
316 different cell lines. Each data set is thus composed of 210 data points of measurements of band intensities
317 already divided by the intensity of the corresponding loading controls, which are total ERK and Akt,
318 respectively. These blots were done using ECL for protein detection and CCD imaging for recording of band
319 intensities. All measurements were detected avoiding overexposure, and as most of the measurements are within

320 a limited dynamic range they are likely within a linear range of detection. Figure 3C illustrates the mean CV
321 obtained for the two data sets after applying different normalisation strategies, and compares these results with
322 the theoretical investigation of Figure 3B. The results obtained with the experimental data agree with the
323 theoretical investigation. The mean CV of the normalised data is relatively low for the normalisation by sum and
324 the normalisation by least squared difference, while higher, on average, for the normalisation by fixed point. In
325 practice, the result of the normalisation by fixed point depends on the choice of the normalisation point, yielding
326 normalised data with low and high variability depending on such choice. In the next section we investigate how
327 to choose a normalisation point.

328 **Low Intensity Data Points are Unsuitable Normalisation Points**

329 In this section we investigate how, in the normalisation by fixed point, the choice of the normalisation point
330 affects the variability of the data. In Figure 3D we illustrate how an increase in the CV of the normalisation
331 point (Condition 1) induces a monotonic increase in the CV of the distribution of the normalised data (Condition
332 2), estimated using Equation (3). This result implies that the CV of the data normalised by fixed point is directly
333 correlated with the CV of the particular condition used as normalisation point. This result also implies that a
334 good choice for a normalisation point is a condition that presents a response with low CV, and hence low
335 uncertainty. Although for non-comparable biological replicates it is impossible to pinpoint which data points
336 have low variability, in the following we provide evidence that low protein band intensities usually yield
337 normalised data with high variability.

338 For this analysis we again use the Western blot data published in the Supplementary Figure S3 of [25]. For both
339 ppERK and pAkt data sets we use each data point as normalisation point and calculate the average CV of the
340 other points resulting from this normalisation. The results are illustrated in Figure 4 where, using a regression by
341 spline functions, we show that choosing low intensity bands as a normalisation point causes an increase in the
342 mean CV of the normalised data. Additionally, because of the result in Figure 3D, we can infer that low
343 intensity bands have usually a larger CV and thus a higher uncertainty. This is most likely due to the low signal-
344 to-noise ratio or, in other words, due to the presence of background noise and the difficulty to separate this noise
345 from low intensity measurements.

346 In addition, we investigated whether the presence of data points that are outside the linear range of detection
347 could also affect the choice of normalisation point. We performed an analysis analogous to what we described
348 above for Figure 4 using the data from the three replicates of the dilution experiments illustrated in Figure 2 and
349 Supporting Information Figures S1, S2 and S3. We used the data of the ECL with CCD imager detection
350 system, which all present non-linearity outside the 32 fold linear range. The results for proteins BSA, RSK1 and
351 mTOR present similarities with what we have found for ppERK and pAkt in Figure 4, i.e. using lower intensity
352 measurements as normalisation point induces larger CV. The result for ERK is shown in Supporting Information
353 Figure S8 and indicates that in this case both high intensity and low intensity normalisation points induce high
354 CV, while medium intensity measurements induce the smallest CV. This is most likely due to the fact that the
355 hyperbolic part of the dilution curves, which is composed of high intensity bands, is not reproduced consistently
356 across replicates. Thus, the variability of high intensity data that are outside the linear range can induce
357 normalised data with large CV even when a high intensity measurement is used as normalisation point.

358 **Impact of Normalisation on Statistical Testing**

359 In this section we use a simulated scenario to investigate the effects of normalisation on the statistical testing
360 applied to examine the significance of differences between protein bands detected by Western blotting. In
361 particular, we test how normalisations influence the sensitivity and specificity of the two-tailed t-test [5], which
362 is frequently used. In order to evaluate the sensitivity and the specificity, we estimate the percentage of false
363 positives and false negatives by repeated data sampling.

364 It is standard practice to employ the t-test in spite of the fact that the actual distribution of Western blot data is
365 unknown and theoretical investigation points toward a log-normal distribution [21], which is different from the
366 normal distribution assumed in the test. Fortunately, the t-test is robust with respect to this violation of its

367 assumptions [26,27] having enabled its widespread application to Western blot data. As we want our analysis to
368 be relevant for the practitioners we therefore comply with the established practice, and also use the t-test.

369 In Figures 5A,B, the row labelled “Before normalisation” illustrates the expected percentage of false positives
370 and false negatives obtained applying the t-test to data distributed as described in the previous figures. Because
371 we set a threshold p-value of 0.05 in the t-test, the percentage of false positive is about 5%, as expected.
372 Variations to the percentage of false positives and false negatives should be attributed to the application of the
373 normalisations.

374 Normalisation by fixed point reduces the percentage of false positives, but greatly increases the percentage of
375 false negatives, i.e. the specificity of the test is increased but the sensitivity is greatly reduced. This result is in
376 agreement with our finding that the normalisation by fixed point increases the CV of the data. Thus, choosing
377 this normalisation method will fail to identify some of the differences between data points. Normalisation by
378 sum affects the percentage of false positives and false negatives in a way that is dependent on the mean of the
379 response to the conditions tested. If relatively low values are tested, e.g. Conditions 2 and 3 in Figures 5A,B, the
380 number of false positives decreases and the number of false negatives increases, while if relatively high values
381 are tested, e.g. Conditions 7 and 8, the number of false positives increases and the number of false negatives
382 decreases. Normalisation by least squared difference also affects false positives and false negatives depending
383 on the magnitude of the data tested. Additionally, it seems that the normalisations by optimal alignment, such as
384 by least squared difference, induce a stronger change in the sensitivity and specificity than the normalisation by
385 sum. In general, normalisation by sum and by optimal alignment can introduce false positives when testing data
386 with values relatively higher than the rest of the data set, reducing the specificity of the test.

387

388 **Discussion**

389 In this paper we have investigated two issues that are important for the quantitative use of Western blot data, i.e.
390 linearity of the detection system and the influence of data normalisations. Our results indicate that for
391 quantitative Western blotting, if the measured intensities vary more than 4-8 fold, then the ECL detected by
392 CCD imager system is preferable to ECL detected by X-ray film, as it yields a larger linear dynamic range. The
393 linear range in the case of ECL in combination with CCD imager spans about 32 fold concentration change for
394 four different proteins with different molecular mass, (Figure 2 and Supporting Information Figures S1, S2 and
395 S3). When we tested fluorescent secondary antibodies detected by the LI-COR scanner, we found that a linear
396 range is similar to the ECL with CCD imager detection method (Supporting Information Figure S4).

397 To better understand the mechanisms behind the normalisation of Western blot data, we use a formalisation
398 based on statistical arguments of three normalisation strategies. Our findings reveal that the normalisation by
399 fixed point introduces additional variability in the data (Figure 3B), and that conditions that induce responses
400 with low CV are preferable normalisation points, because they induce a lower CV of the normalised data
401 (Figure 3D). Although the CV of the response to specific conditions is in general not known, we provide
402 evidence of whether low, medium or high intensity measurements have usually high or low CV. In particular we
403 showed that low intensity measurements are usually inappropriate normalisation points (Figure 4). This is most
404 likely due to the low signal-to-noise ratio and consequent high CV of low intensity measurements. Additionally,
405 we showed that high intensity measurements that are outside the linear dynamic range are inappropriate
406 normalisation points (Supporting Information Figure S8). Therefore, we suggest that for this type of
407 normalisation the most appropriate normalisation points are data points with medium intensity measurements.
408 Because the normalisation by fixed point increases the CV of the normalised data, this also has an impact on
409 statistical testing. When applying a two-tailed t-test to the normalised data, we saw an increase in the specificity
410 of the test and a strong decrease of the sensitivity (Figure 5A,B). While a high specificity is desirable, the
411 decline in sensitivity increases the chances of overlooking significant differences between data points. In
412 addition, if the normalisation point is not chosen carefully, the normalised data could present a high variability
413 and it might become very difficult to detect when two conditions yield different results.

414 The normalisations by sum and by optimal alignment also influence the variability of the normalised data.
415 Rather than introducing uncertainty, in this case the uncertainty is redistributed depending on the relative
416 magnitude of the measurements (Figures 3A and 3B). In particular, the variability of high intensity
417 measurements is reduced, while the variability of low intensity measurements is increased. This redistribution is
418 due to the fact that normalised data points depend on the data points from other conditions or even from other
419 replicates, as highlighted by the random variable of the normalised data in Equation (5) and Equation (S5) in
420 Supporting Information S1.

421 A consequence of this redistribution is also that normalisations by sum and by optimal alignment have an impact
422 on statistical testing. By applying a two-tailed t-test we observed an increase in sensitivity and decrease in
423 specificity, when testing conditions with high intensity measurements (Figures 5A,B). Because more false
424 positives are detected, the distinction of differences between two data points with high intensity measurements
425 becomes less reliable than before normalisation. The alterations of sensitivity and specificity are inverted when
426 data points with low intensity measurements are tested. These results imply that when these normalisations are
427 applied, it is necessary to pay attention to whether high intensity or low intensity data points are tested and
428 interpret the results accordingly. It is also possible to envision the definition of a data transformation or
429 modified t-test to tune sensitivity and specificity based on the relative magnitude of the measurements tested,
430 and calibrate the number of false positives to 5% of the cases.

431 Our findings also have implications for the use of Western blot data for mathematical model training and
432 validation. In this setting, data is compared to the output of a model and appropriate values for the parameters of
433 the model are identified, aiming to obtain the best possible agreement between data and output [4]. Because data
434 normalisation has an influence on the distribution of the normalised data, we advise to normalise also the model
435 output before comparing it to the data, when the nature of the mathematical model permits it. This should allow
436 for a fair comparison between output and data, because in principle they would be subject to the same data
437 transformation.

438 Although the quantitative use of Western blotting is now widespread, published articles often lack the details of
439 how Western blot results were quantified and how biological replicates were compared to obtain statistics [23].
440 We hope that the results in this paper will serve as a reference and encourage scientists to include in future
441 publications what we demonstrate to be critical information. To this end, based on our results, we wrote a short
442 manual of one page that contains a step-by-step guide to help biologists choose the normalisation strategy that is
443 the most appropriate to their case. This manual can be found in Supporting Information S2.

444

445 **Acknowledgements**

446 We would like to thank Dr. Maria Luisa Guerriero for the helpful discussion.

447

448 **References**

- 449 1. Burnette WN (1981) "Western blotting": electrophoretic transfer of proteins from sodium dodecyl sulfate--
450 polyacrylamide gels to unmodified nitrocellulose and radiographic detection with antibody and
451 radioiodinated protein A. *Anal Biochem* 112: 195-203.
- 452 2. Towbin H, Staehelin T, Gordon J (1979) Electrophoretic transfer of proteins from polyacrylamide gels to
453 nitrocellulose sheets: procedure and some applications. *Proc Natl Acad Sci U S A* 76: 4350-4354.
- 454 3. Kitano H (2002) Computational systems biology. *Nature* 420: 206-210.
- 455 4. Maiwald T, Timmer J (2008) Dynamical modeling and multi-experiment fitting with PottersWheel.
456 *Bioinformatics* 24: 2037-2043.
- 457 5. Zar J (1998) *Biostatistical Analysis* (4th Edition): {Prentice Hall}.
- 458 6. Wang YV, Wade M, Wong E, Li YC, Rodewald LW, et al. (2007) Quantitative analyses reveal the
459 importance of regulated Hdmx degradation for p53 activation. *Proc Natl Acad Sci U S A* 104: 12365-
460 12370.

- 461 7. Heidebrecht F, Heidebrecht A, Schulz I, Behrens SE, Bader A (2009) Improved semiquantitative Western
462 blot technique with increased quantification range. *Journal of Immunological Methods* 345: 40-48.
- 463 8. Speed TP (2003) *Statistical analysis of gene expression microarray data*. Boca Raton, FL: Chapman &
464 Hall/CRC. xiii, 222 p., 224 p. of plates p.
- 465 9. Bolstad BM, Irizarry RA, Astrand M, Speed TP (2003) A comparison of normalization methods for high
466 density oligonucleotide array data based on variance and bias. *Bioinformatics* 19: 185-193.
- 467 10. Li C, Wong WH (2001) Model-based analysis of oligonucleotide arrays: expression index computation and
468 outlier detection. *Proc Natl Acad Sci U S A* 98: 31-36.
- 469 11. Zhang R, Yang D, Zhou C, Cheng K, Liu Z, et al. (2012) beta-actin as a loading control for plasma-based
470 Western blot analysis of major depressive disorder patients. *Anal Biochem* 427: 116-120.
- 471 12. Liu NK, Xu XM (2006) beta-tubulin is a more suitable internal control than beta-actin in western blot
472 analysis of spinal cord tissues after traumatic injury. *J Neurotrauma* 23: 1794-1801.
- 473 13. Wu Y, Wu M, He G, Zhang X, Li W, et al. (2012) Glyceraldehyde-3-phosphate dehydrogenase: a universal
474 internal control for Western blots in prokaryotic and eukaryotic cells. *Anal Biochem* 423: 15-22.
- 475 14. Bruning U, Fitzpatrick SF, Frank T, Birtwistle M, Taylor CT, et al. (2012) NFkappaB and HIF display
476 synergistic behaviour during hypoxic inflammation. *Cell Mol Life Sci* 69: 1319-1329.
- 477 15. Lange F, Rateitschak K, Fitzner B, Pohland R, Wolkenhauer O, et al. (2011) Studies on mechanisms of
478 interferon-gamma action in pancreatic cancer using a data-driven and model-based approach. *Mol*
479 *Cancer* 10: 13.
- 480 16. Witt J, Konrath F, Sawodny O, Ederer M, Kulms D, et al. (2012) Analysing the role of UVB-induced
481 translational inhibition and PP2Ac deactivation in NF-kappaB signalling using a minimal mathematical
482 model. *PLoS One* 7: e40274.
- 483 17. Neumann L, Pforr C, Beaudouin J, Pappa A, Fricker N, et al. (2010) Dynamics within the CD95 death-
484 inducing signaling complex decide life and death of cells. *Mol Syst Biol* 6.
- 485 18. Wang CC, Cirit M, Haugh JM (2009) PI3K-dependent cross-talk interactions converge with Ras as
486 quantifiable inputs integrated by Erk. *Mol Syst Biol* 5: 246.
- 487 19. Schilling M, Maiwald T, Bohl S, Kollmann M, Kreutz C, et al. (2005) Computational processing and error
488 reduction strategies for standardized quantitative data in biological networks. *FEBS J* 272: 6400-6411.
- 489 20. Aksamitiene E, Hoek JB, Kholodenko B, Kiyatkin A (2007) Multistrip Western blotting to increase
490 quantitative data output. *Electrophoresis* 28: 3163-3173.
- 491 21. Kreutz C, Bartolome Rodriguez MM, Maiwald T, Seidl M, Blum HE, et al. (2007) An error model for
492 protein quantification. *Bioinformatics* 23: 2747-2753.
- 493 22. Rocke DM, Durbin B (2001) A model for measurement error for gene expression arrays. *J Comput Biol* 8:
494 557-569.
- 495 23. Gassmann M, Grenacher B, Rohde B, Vogel J (2009) Quantifying Western blots: pitfalls of densitometry.
496 *Electrophoresis* 30: 1845-1855.
- 497 24. Box GEP, Muller ME (1958) A Note on the Generation of Random Normal Deviates. *Annals of*
498 *Mathematical Statistics* 29: 610-611.
- 499 25. Rauch J, Kolch W, Mahmoudi M (2012) Cell Type-Specific Activation of AKT and ERK Signaling
500 Pathways by Small Negatively-Charged Magnetic Nanoparticles. *Sci Rep* 2.
- 501 26. Bartlett MS (1935) The Effect of Non-Normality on the t Distribution. *Mathematical Proceedings of the*
502 *Cambridge Philosophical Society* 31: 223-231.
- 503 27. Boneau CA (1960) The effects of violations of assumptions underlying the test. *Psychol Bull* 57: 49-64.

504

505

506 **Figure Legends**

507 **Figure 1. Normalisations of Western blot replicates in the literature.** We divide the normalisations found in
508 literature into three categories: (A) normalisation by fixed normalisation point or control; (B) normalisation by
509 sum of the replicate; (C) normalisation by optimal alignment. For illustration purposes we do not use actual
510 Western blot data. Each normalisation is presented using three cartoon Western blots, representing three
511 replicates, and highlighting with red circles the data points used in the normalisation procedure. The graphs
512 show the normalised data, where the points belonging to the same replicate are connected with lines.

513 **Figure 2. Signal linearity obtained by different Western blot detection systems.** Representative experiments
514 of Western blots containing 2-fold serial dilution of BSA. Shown are the representative results from 3

515 independent experiments. BSA was detected by (A,C) ECL with X-ray film and (B,D) ECL with CCD imager.
516 Blue squares indicate data points that are linear, while red triangles indicate data points outside the linear range
517 of detection. To highlight linear and non-linear data we use linear trend lines, reporting the coefficient of
518 determination R^2 . In (A,B) data are in log-log scale to improve visualisation.

519 **Figure 3. Effect of the normalisation on the CV of the normalised data.** (A) Distribution of the data in a
520 simulated scenario. In our theoretical analysis of the effects of the normalisation on the variability of the
521 normalised data we consider a distribution of the response to eight conditions. We use log-normal distributions
522 with CV 0.2 and mean of the response to the conditions from 1 to 8 as 1, 2, 3, 4, 7, 10.5, 18, 27. (B) CVs are
523 shown for the distribution of the simulated data before normalisation, after normalisation by first condition, after
524 normalisation by sum of all data points in a replicate and after normalisation by least squared differences. The
525 mean CV is computed as the average across the eight conditions. (C) Data from Supplementary Figure S3 of
526 [25] (Supporting Information Figure S5 in this publication) were normalised using different normalisation
527 strategies and the mean CV of the resulting normalised data is shown. As the mean CV obtained by the
528 normalisation by fixed point depends on the choice of normalisation point, we report the mean and standard
529 deviation obtained. We also report the mean CV obtained using ppERK and pAkt data and we compare them
530 with the theoretical results of Figure 3B. (D) Before normalisation, the response to Condition 2 has a CV of 0.2,
531 as shown in Figure 3A. Condition 2 is then normalised by fixed point, with Condition 1 as normalisation point.
532 Here we show how the CV of normalised Condition 2 changes for increasing CV of the normalisation point
533 Condition 1.

534 **Figure 4. Correlation between the intensity of the normalisation points and the CV of the normalised**
535 **data.** Using data from (A) phosphorylated Akt and (B) phosphorylated ERK from Supplementary Figure S3 in
536 [25] (Supporting Information Figure S5 in this publication) we tested every point on a blot as normalisation
537 point. For each resulting normalisation we computed the average of the CV of the normalised data points, and
538 plotted the value of each data point (scaled so that the maximum of each replicate is equal to 1) against the
539 average CV obtained by normalising with the corresponding data point. The result shows how the intensities of
540 each normalisation point chosen correlate with the variability of the normalised data.

541 **Figure 5. Effects of normalisation on false positives and false negatives when applying t-test for equality**
542 **of the mean.** (A) We consider responses to eight conditions with log-normal distributions with CV of 0.2 and
543 means of the conditions from 1 to 8 equal to: 1, 2, 2, 4, 7, 7, 18, 18. A number $n=5$ of sampled replicates are
544 obtained from these distributions and normalised using the normalisations above. Using these replicates before
545 and after normalisation, conditions are tested using a two-tailed t-test with threshold p-value of 0.05. We repeat
546 this procedure a large number of times and estimate the percentage of false positives. (B) In analogy with (A),
547 we estimate the number of false negatives considering means of the conditions from 1 to 8 equal to: 1, 2, 3, 4, 7,
548 10.5, 18, 27. Notice that for a fair comparison, when testing two conditions, one has a mean that is always $2/3$
549 the mean of the other, e.g. Condition 5 has mean 7 and Condition 6 has mean 10.5, with $7/10.5=2/3$.

550

551 **Figure S1. Signal linearity of ERK obtained by different Western blot detection systems.** Shown are
552 representative results from three independent experiments of Western blots containing 2-fold serial dilution of
553 cell lysate. ERK was detected by (A,C) ECL with X-ray film and (B,D) ECL with CCD imager. Blue squares
554 indicate data points that are linear, while red triangles indicate data points outside the linear range of detection.
555 To highlight linear and non-linear data we use linear trend lines, reporting the coefficient of determination R^2 .
556 In (A,B) data are in log-log scale to improve visualisation.

557 **Figure S2. Signal linearity of RSK1 obtained by different Western blot detection systems.** Shown are
558 representative results from three independent experiments of Western blots containing 2-fold serial dilution of
559 cell lysate. RSK1 was detected by (A,C) ECL with X-ray film and (B,D) ECL with CCD imager. Blue squares
560 indicate data points that are linear, while red triangles indicate data points outside the linear range of detection.

561 To highlight linear and non-linear data we use linear trend lines, reporting the coefficient of determination R^2 .
562 In (A,B) data are in log-log scale to improve visualisation.

563 **Figure S3. Signal linearity of mTOR1 obtained by different Western blot detection systems.** Shown are
564 representative results from three independent experiments of Western blots containing 2-fold serial dilution of
565 cell lysate. Protein mTOR1 was detected by (A,C) ECL with X-ray film and (B,D) ECL with CCD imager. Blue
566 squares indicate data points that are linear, while red triangles indicate data points outside the linear range of
567 detection. To highlight linear and non-linear data we use linear trend lines, reporting the coefficient of
568 determination R^2 . In (A,B) data are in log-log scale to improve visualisation.

569 **Figure S4. Signal linearity of BSA and ERK obtained by fluorescent secondary antibodies.** Shown are
570 representative results from three independent experiments of Western blots containing 2-fold serial dilution of
571 (A,C) BSA and (B,D) cell lysate. BSA and ERK were detected using fluorescent secondary antibodies. Blue
572 squares indicate data points that are linear, while red triangles indicate data points outside the linear range of
573 detection. To highlight linear and non-linear data we use linear trend lines, reporting the coefficient of
574 determination R^2 . In (A,B) data are in log-log scale to improve visualisation.

575

576 **Figure S5. Supplementary Figure S3 of [25].** Experimental data used in Figures 3C and 4. The experiments
577 shown in Figure S5 were performed as described in by Rauch et al. in [25].

578 **Figure S6. Effect of the normalisation on the coefficient of variation of the normalised data.** (A) CVs are
579 shown for the distribution of the simulated data before normalisation, after normalisation by first condition, after
580 normalisation by sum of all data points in a replicate and after normalisation by least squared differences. The
581 mean coefficient of variation is computed as the average across the eight conditions. Mean and standard
582 deviation of the data before normalisation is given in Figure 3A of the main text, and here is normally
583 distributed. (B) Before normalisation, the response to Condition 2 has a coefficient of variation of 0.2, as shown
584 in Figure 3A of the main text. Condition 2 is then normalised by fixed point, with Condition 1 as normalisation
585 point. Here we show how the coefficient of variation of normalised Condition 2 changes for increasing
586 coefficient of variation of the normalisation point Condition 1.

587

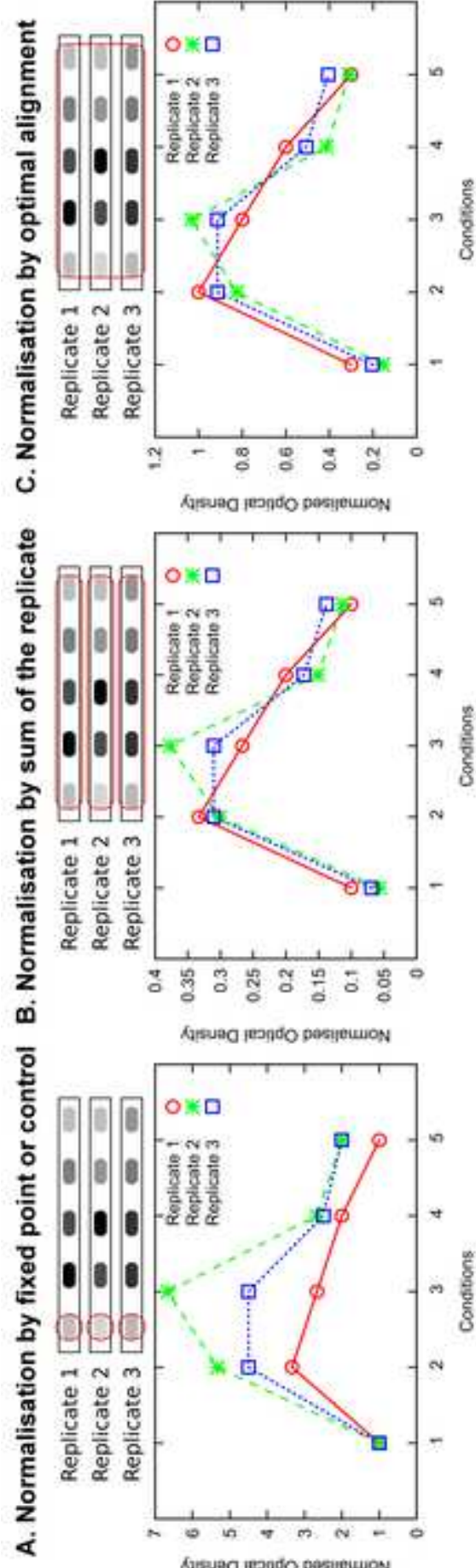
588 **Figure S7. Effects of normalisation on false positives and false negatives when applying t-test for equality
589 of the mean.** (A) We consider responses to eight conditions with normal distributions with CV of 0.2 and means
590 of the conditions from 1 to 8 equal to: 1, 2, 2, 4, 7, 7, 18, 18. A number $n=5$ of sampled replicates are obtained
591 from these distributions and normalised using the normalisations above. Using these replicates before and after
592 normalisation, conditions are tested using a two-tailed t-test with threshold p-value of 0.05. We repeat this
593 procedure a large number of times and estimate the percentage of false positives. (B) In analogy with (A), we
594 estimate the number of false negatives considering means of the conditions from 1 to 8 equal to: 1, 2, 3, 4, 7,
595 10.5, 18, 27. Notice that for a fair comparison, when testing two conditions, one has a mean that is always $2/3$
596 the mean of the other, e.g. Condition 5 has mean 7 and Condition 6 has mean 10.5, with $7/10.5=2/3$.

597

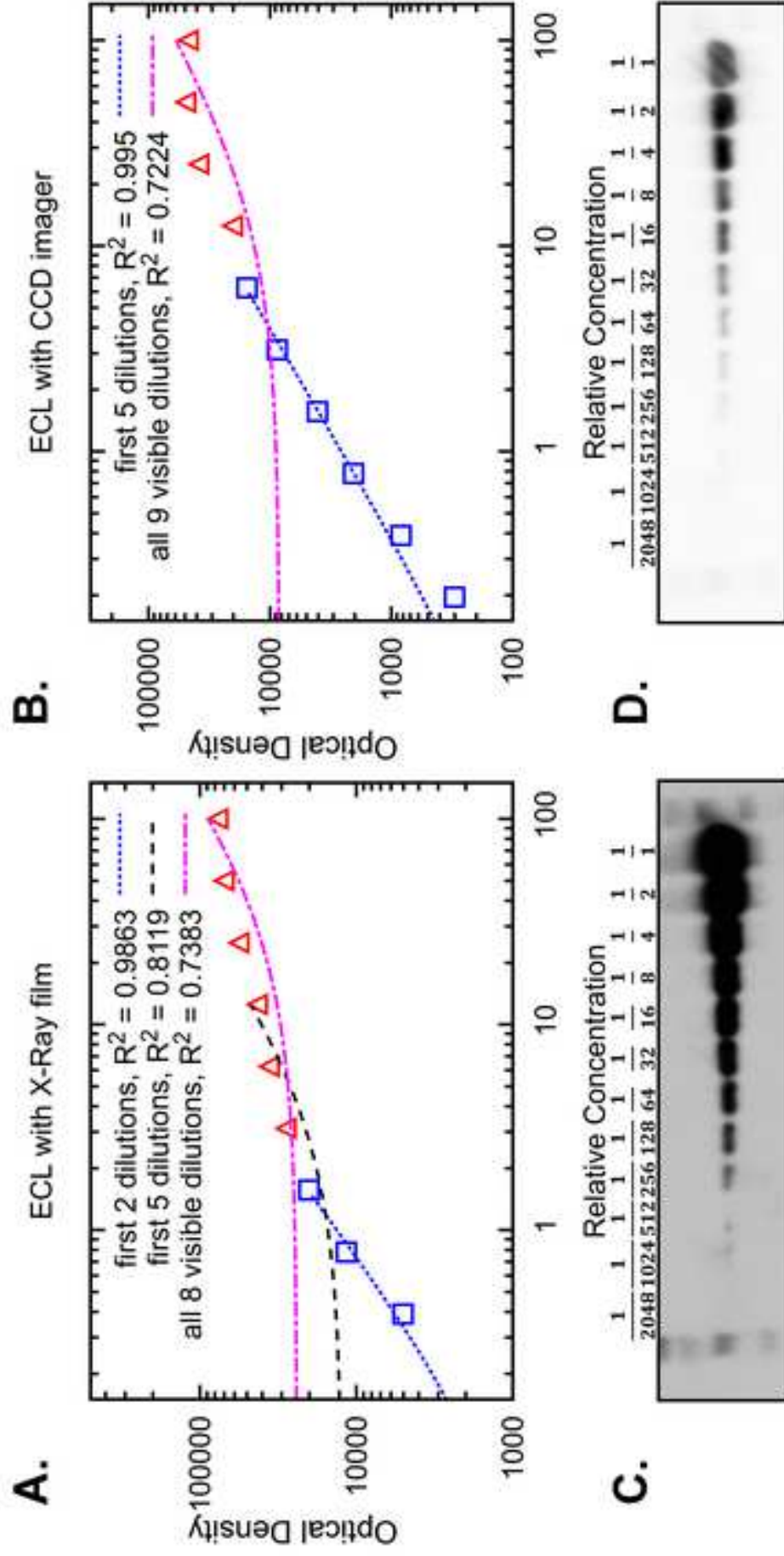
598 **Figure S8. Correlation between the intensity of the normalisation points and the CV of the normalised
599 data.** Using data from the three replicates of the ERK dilution experiments detected with CCD imager, we
600 tested every point on a blot as normalisation point. For each resulting normalisation we computed the average of
601 the CV of the normalised data points, and plotted the value of each data point (scaled so that the maximum of
602 each replicate is equal to 1) against the average CV obtained by normalising with the corresponding data point.
603 The result shows how the intensities of each normalisation point chosen correlate with the variability of the
604 normalised data.

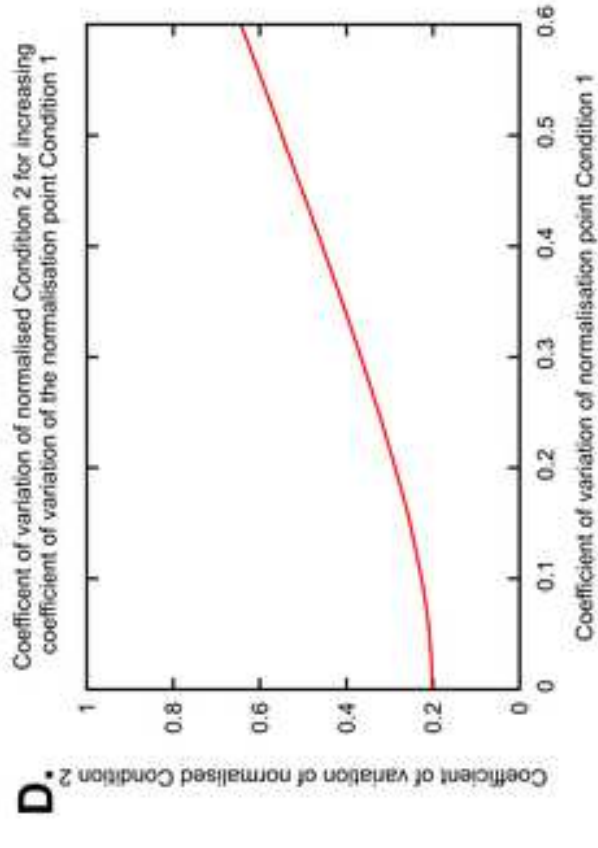
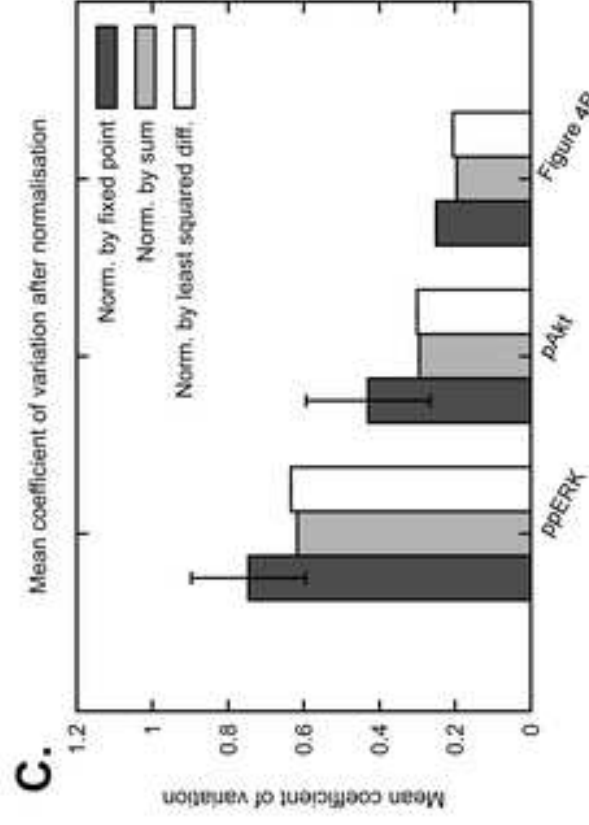
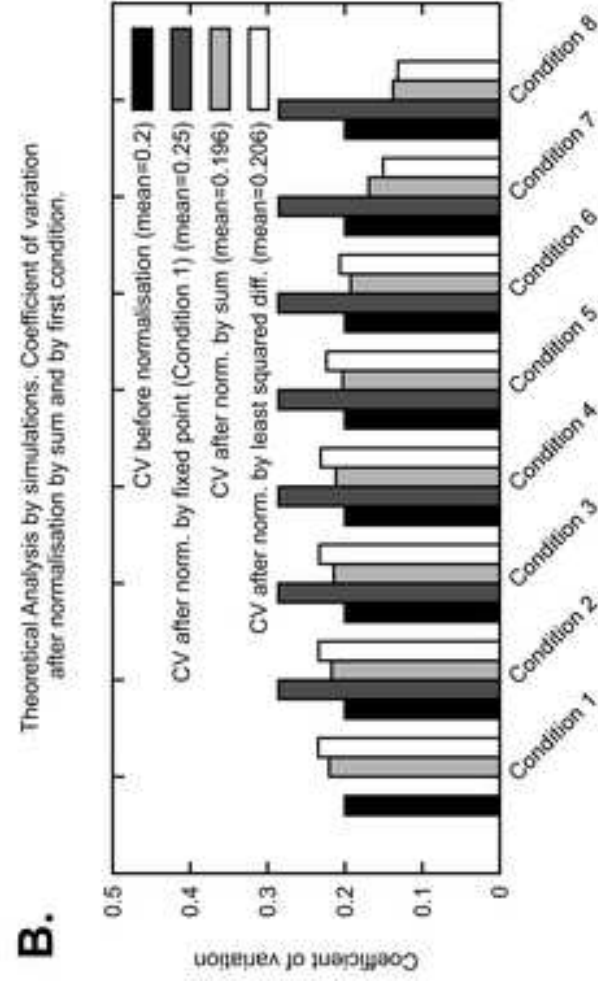
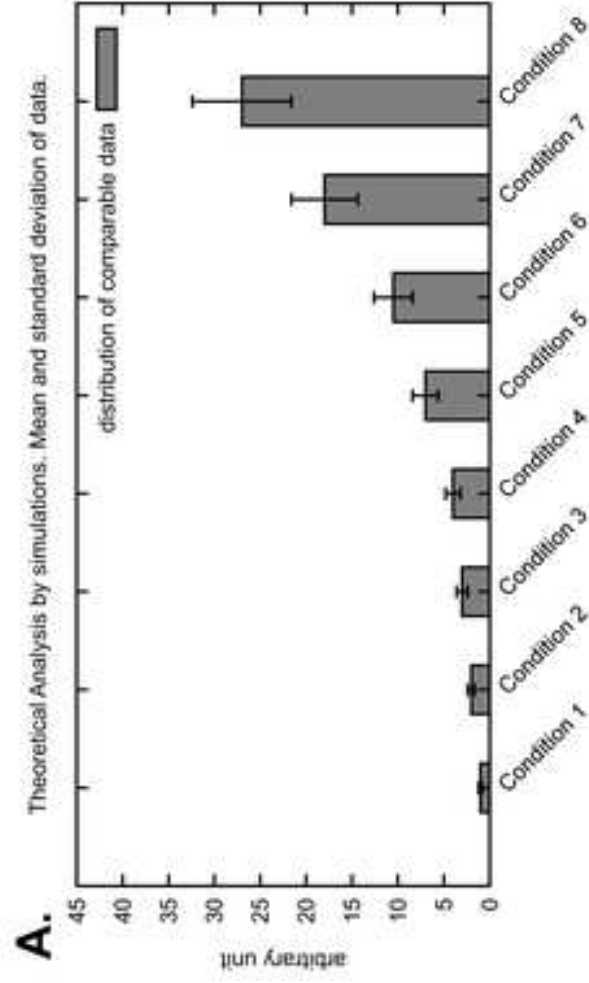
Figure 1

[Click here to download high resolution image](#)



Dilution experiments BSA: representative experiments





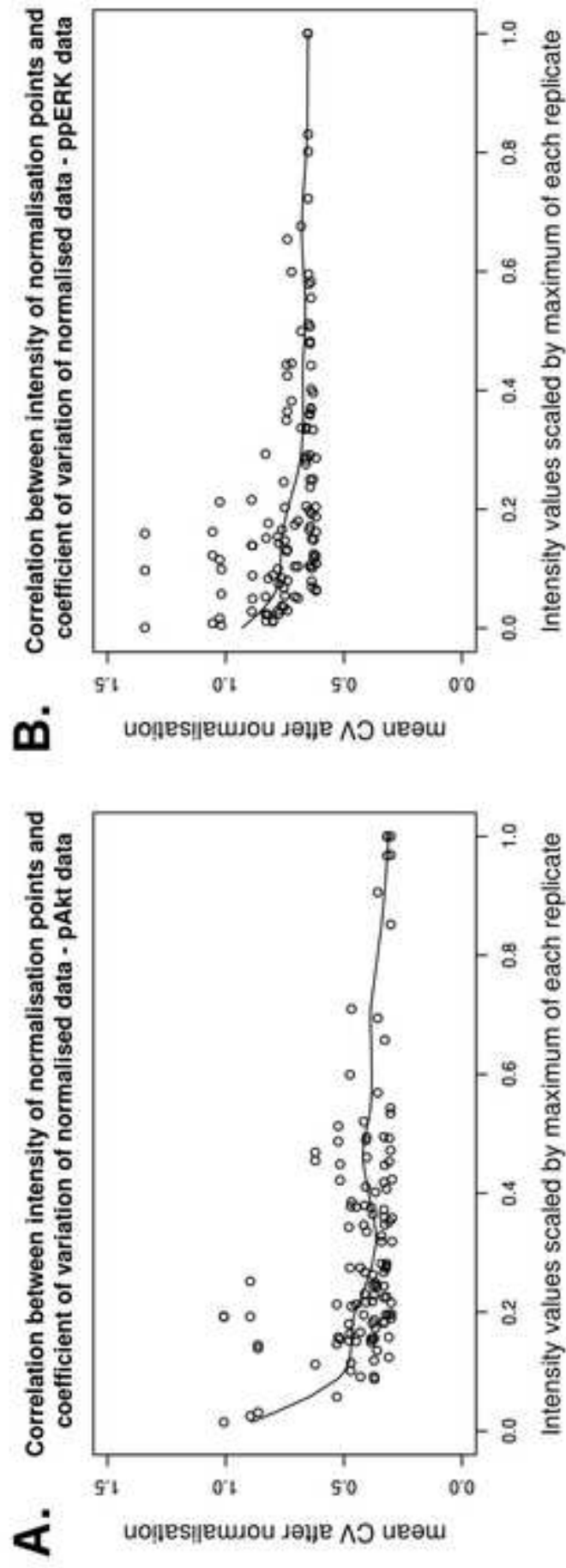


Figure 5
[Click here to download high resolution image](#)

